

# Time-Since-Infection Model for Hospitalization and Incidence Data

JIASHENG SHI, YIZHAO ZHOU, JING HUANG\*

*Department of Biostatistics, Epidemiology, and Informatics, Perelman School of Medicine,  
University of Pennsylvania, Philadelphia, USA*

jing14@pennmedicine.upenn.edu

## SUMMARY

The Time Since Infection (TSI) models, which use disease surveillance data to model infectious diseases, have become increasingly popular recently due to their flexibility and capacity to address complex disease control questions. However, a notable limitation of TSI models is their primary reliance on incidence data. Even when hospitalization data are available, existing TSI models have not been crafted to estimate disease transmission or predict disease-related hospitalizations - metrics crucial for understanding a pandemic and planning hospital resources. Moreover, their dependence on reported infection data makes them vulnerable to variations in data quality. In this study, we advance TSI models by integrating hospitalization data, marking a significant step forward in modeling with TSI models. Our improvements enable the estimation of key infectious disease parameters without relying on contact tracing data, reduce bias in incidence data, and provide a foundation to connect TSI models with other infectious disease models. We introduce hospitalization propensity parameters to jointly model incidence and hospitalization data. We use a composite likelihood function to accommodate complex data structure and an MCEM algorithm to estimate model parameters. We apply our method to COVID-19 data to estimate disease transmission, assess risk factor impacts, and calculate hospitalization propensity.

\*To whom correspondence should be addressed.

*Key words:* Composite likelihood function; Hospitalization propensity; Infectious disease transmission; Time between diagnosis and hospitalization.

## 1. INTRODUCTION

Mathematical modeling plays a crucial role in comprehending infectious disease transmission. By estimating essential transmission parameters, predicting epidemic trends, and enabling real-time comparisons of response strategies, quantitative models transform information about disease processes into actionable statistics. In the early stages of novel pandemics, when vaccines and treatments are unavailable, and the entire population lacks immunity, policymakers often rely on a selected set of key statistics to make timely and effective decisions. These statistics include but are not limited to, the effective reproduction number ( $R_t$ ), projected incidence counts, projected hospitalization counts, and the impact of intervenable factors. A plethora of modeling approaches have been developed to estimate these statistics, particularly in response to the COVID-19 pandemic, each with its unique advantages and limitations. These models encompass a range of methodologies, including compartmental models, agent-based simulations, time-series analyses, and network-based approaches. Within this field, one noteworthy category is the Time Since Infection (TSI) models.

The concept of Time since Infection (TSI) models can be traced back to the work of Ross and Hudson in the 1910s Ross (1916); Ross and Hudson (1917*a,b*). Their mathematical basis was described in a seminal paper by Kermack and McKendrick in 1927 Kermack and McKendrick (1927) and was formally formulated and gained more prominence with Wallinga's work in 2004 and Fraser's contributions in 2007 Wallinga and Teunis (2004); Fraser (2007). The models then gained further recognition in the statistics community following Cori's work in 2013 Cori *and others* (2013). Thanks to Cori's development of an R package named EpiEstim Cori (2021), these models have been increasingly employed to estimate real-time disease transmission rates over the past decade. During the COVID-19 pandemic, TSI models were extensively used to analyze the

pandemic (Pan *and others*, 2020; Nouvellet *and others*, 2021; Amman *and others*, 2022; Nash *and others*, 2022; Ge *and others*, 2023) and demonstrated superior accuracy in estimating  $R_t$  compared to many other methods (Gostic *and others*, 2020; Nash *and others*, 2022). Moreover, building upon the original TSI models, researchers have proposed several enhancements that either relax model assumptions or address challenges with real data. These improvements include integrating TSI models with regression models, addressing reporting delays and underreporting, refining the estimation of serial interval distributions, and enabling the simultaneous analysis of multiple locations, among other innovations (Wilder *and others*, 2021; Salas, 2021; Quick *and others*, 2021; Shi *and others*, 2022; Ge *and others*, 2023).

The TSI models are designed around the premise that the number of new infections at a particular moment is influenced by three primary factors: the count of recent infections, the reproduction number at that moment, and an infectiousness function that measures the contagiousness of an infected person at each time since infection. For illustration, consider discrete time by day and let  $I_t$  represent the number of newly infected individuals on day  $t$ . If we know the number of infections before day  $t$ , denoted by  $I_0, \dots, I_{t-1}$ , the expected number of new infections on day  $t$  is written as the multiplication of the instantaneous reproduction number and the infection potential on that particular day. This relationship can be expressed as  $E(I_t | I_0, \dots, I_{t-1}) = R_t \Lambda_t$ , where  $\Lambda_t \triangleq \sum_{s=1}^t I_{t-s} \omega_s$  stands for the infection potential on day  $t$ . It is shaped by the current number of infectious individuals and the infectiousness function  $\omega_s$ , which quantifies the infectiousness of the existing infectious individuals on the  $s$ -th day after infection, with  $\sum_{s=0}^{+\infty} \omega_s = 1$ . Practically, we can assume  $\omega_s = 0$  for  $s = 0$  and  $s > \eta$  with  $\eta$  being the duration between infection and recovery. This infectiousness function can be approximated using the probability distribution of the serial interval or generation time (Svensson, 2007). To estimate  $R_t$ , one may assume distribution assumptions for  $I_t$  and use methods like maximum likelihood or Bayesian approaches with predetermined values of  $\omega_s$  (Cori *and others*, 2013; WHO Ebola Response Team,

2014; Quick *and others*, 2021).

Compared to other methods, TSI models stand out due to their practicality and flexibility. Being statistical in nature, the models can be integrated with advanced statistical structures, offering significant potential for modeling complex questions (Quick *and others*, 2021; Shi *and others*, 2022; Nash *and others*, 2022). The models are empirical, suggesting that they can be practically applied with a reasonable understanding of how available data are generated, even without a detailed epidemiological understanding of transmission characteristics (Jewell, 2021). This makes them highly useful for modeling outbreaks caused by novel infectious pathogens. Most notably, TSI models only require incidence data to estimate  $R_t$ . This simplicity ensures the models are easy to estimate and remain user-friendly, even when other disease surveillance data are unavailable. This characteristic is particularly attractive during the early stages of pandemics when national disease surveillance systems are still developing. However, a significant weakness of the TSI model also stems from this reliance. Since they primarily rely on incidence data, even when hospital data become available, the original TSI models cannot model or predict disease-related hospitalizations, a crucial statistic for evaluating a pandemic's trajectory and for hospital planning. Additionally, this reliance also makes the models susceptible to fluctuations in the quality of reported infection data.

In this study, we focus on advancing the framework of TSI models by incorporating a critical yet overlooked aspect: the modeling of hospitalization data. This inclusion represents a significant step forward in infectious disease modeling using TSI models, with profound implications for both research and practical applications. Our motivation for this advancement is threefold. First, it enables the modeling of hospitalizations, an indispensable tool for managing healthcare resources during epidemics. As shown in our data application, the proposed method allows estimation of key hospitalization related parameters without using contacting tracing data which are often difficult to obtain. Second, it helps reduce bias stemming from errors in incidence data,

leading to a more accurate representation of disease dynamics. Third, from a model development perspective, integrating both hospitalization and incidence data into the models could allow us to draw connections and unify the strengths of TSI models with other infectious disease models, such as compartmental models, given their common heritage.

While the potential benefits of incorporating hospitalization data into TSI models are clear, the technical challenges posed by this endeavor are non-trivial. To jointly model incidence and hospitalization counts, we introduce a new set of parameters, similar to the infectiousness function, named hospitalization propensity,  $\tilde{\omega}_s$ , which quantifies the tendency of infectious individuals being hospitalized on the  $s$ -th day after infection. These parameters can be approximated using the probability distribution of the time between disease onset and hospitalization, or they can be estimated directly from the proposed model. The relationship between the incidence data and the hospitalization data is then linked using the hospitalization propensity. However, specifying the joint likelihood function is challenging due to the complicated recurrence relation between incidence and hospitalization data. To address this, we propose using a composite likelihood function, providing a flexible and robust way to accommodate complex structures inherent in the hospitalization and incidence data. We develop an MCEM algorithm to estimate the model parameters and derive the asymptotic properties of the estimators. We evaluate the performance of our model through simulation studies and study its robustness by conducting sensitivity analyses in a range of scenarios of misspecified models. We apply the proposed methods to analyze county-level COVID-19 daily confirmed infection counts, and hospitalization data across the U.S. in 2021, estimating the reproductive numbers, and the impact of local-level risk factors on disease transmission. In the following sections, we delve into the details of our novel TSI model, elucidating its key components and demonstrating its advantages through empirical analyses. Our goal is to contribute to the ongoing discourse in infectious disease modeling, offering a fresh perspective on leveraging hospitalization data to enhance our understanding of disease dynamics

and strengthen public health efforts.

## 2. MODEL

### 2.1 *Model and Notations*

We use subscripts  $t$  to denote calendar time and  $s$  to indicate time since infection. By “hospitalization”, we refer to hospital admission due to the infectious disease. Here, we consider discrete time. Let  $I_t$  represent the number of new infections and  $H_t$  denote the number of new hospitalizations at time  $t$ . We define the filtrations  $\mathcal{F}_t = \sigma(\{I_r, 0 \leq r \leq t\})$  and  $\mathcal{G}_t = \sigma(\{I_r, H_r, 0 \leq r \leq t\})$  which represent the information on past infections and the combined information on both past infections and hospitalizations, respectively. In line with the original TSI models, we assume the number of new infections at time  $t$ , given the number of previously infected individuals, follows a Poisson distribution:

$$I_t \mid \mathcal{F}_{t-1} \sim \text{Poisson}(R_t \Lambda_t), \quad (2.1)$$

Next, we denote  $h_{t,s}$  as the number of patients infected at calendar time  $t$  and admitted at calendar time  $t + s$ , i.e., time  $s$  since infection. We assume the hospitalization propensity of an infected individual,  $\tilde{\omega}_s$ , describes the tendency of infectious individuals to be hospitalized on the  $s$ -th time after infection and it is independent of the calendar time  $t$ . Then, the expected value of  $h_{t,s}$  can be expressed as  $\mathbb{E}(h_{t,s} \mid \mathcal{F}_t) = \tilde{\omega}_s I_t$ . In practice, we can assume that if an infected individual is not hospitalized within a certain period after their infection, their hospitalization propensity approaches zero. We then set  $h_{t,s} = 0$  and  $\tilde{\omega}_s = 0$  for  $s > \tilde{\eta}$  for all  $t$ , where the positive integer  $\tilde{\eta}$  represents the duration from infection to the time after which the likelihood of hospitalization becomes negligible. We also define  $h_{t,-1}$  as the total number of patients infected at time  $t$  who will never be hospitalized due to the infection and set the tendency  $\tilde{\omega}_{-1} = 1 - \sum_{s=0}^{\tilde{\eta}} \tilde{\omega}_s$ . Thus, the total incidence at time  $t$  is equal to the sum of patients who were infected at calendar time  $t$  and admitted at time  $s$  since infection, plus those infected at calendar time  $t$  and never

hospitalized. The total hospitalizations at time  $t$  is the sum of patients who were infected at calendar time  $t - s$  and admitted at time  $s$  since infection. In this way, the relationship between disease incidence and hospitalization is connected through

$$I_t = h_{t,-1} + \sum_{s \geq 0} h_{t,s}, \text{ and } H_t = \sum_{s=0}^t h_{t-s,s}, \text{ for } t = 0, 1, 2, \dots \quad (2.2)$$

Based on the above setup, we further assume

$$(h_{t,-1}, h_{t,0}, \dots, h_{t,\bar{\eta}}) | I_t \sim \text{Multinomial}(I_t, \tilde{\omega}_{-1}, \tilde{\omega}_0, \dots, \tilde{\omega}_{\bar{\eta}}). \quad (2.3)$$

From Equations (2.2) and (2.3), we can see that the time-series data of daily infections and hospitalizations exhibit deeply connected, crossover, and overlapping structures. This intricate relationship is illustrated in two plots, as shown in Figure 1.

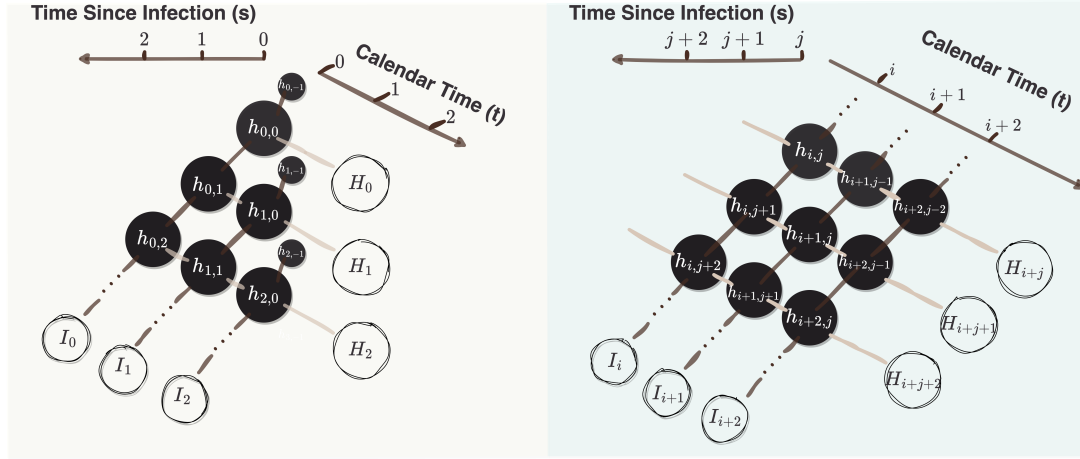


Fig. 1. The relationship between incidence data  $I_t$  and hospitalization data  $H_t$ . The left panel illustrates the relationship between calendar time 0 and 2 and time since infection from 0 to 2. The right panel illustrates the relationship between calendar time  $i$  and  $i + 2$  and time since infection from  $j$  to  $j + 2$ .

Furthermore, to model the impact of risk factors on  $R_t$ , we draw inspiration from Shi *and others* (2022); Quick *and others* (2021) and Zeger and Qaqish (1988) to assume a regression

structure in which:

$$h(R_t) = X_t^T \beta + \sum_{i=1}^q \theta_i f_i(D_{1,t}, D_{2,t}, D_{3,t}), \quad (2.4)$$

where  $t \geq q > 0$  and  $X_t$  is a  $p$ -dimensional vector that includes a constant 1 and a vector of risk factors of disease transmission,  $Z_t$ , such as temperature, social distancing measures, and population density. In this equation,  $h(\cdot)$  and  $f_i(\cdot)$  represent a known link function and functions of past outcomes, respectively. Additionally,

$$D_{1,t} = \{X_r\}_{0 \leq r \leq t}, \quad D_{2,t} = \{I_r, \mathbb{E}(H_r)\}_{0 \leq r \leq t-1}, \quad D_{3,t} = \{R_r\}_{0 \leq r \leq t-1}. \quad (2.5)$$

Assuming  $D_{1,t}$  is observed, (2.4) ensures  $R_t \in \mathcal{F}_t$ . By combining (2.1)-(2.5), we build a TSI model for hospitalization and incidence data. Indeed, the terms  $\{\mathbb{E}(H_r)\}_{1 \leq r \leq t-1}$  in  $D_{2,t}$  can be expressed as functions of the hospitalization propensity and the  $R_t$  according to our model. This implies that  $D_{2,t} \subset \sigma(\{I_r, R_r\}_{0 \leq r \leq t-1})$  and hospitalization data are linked with the disease transmission through the hospitalization propensity. In a broader context, one could substitute  $D_{2,t}$  in (2.5) with  $\{I_r, H_r\}_{0 \leq r \leq t-1}$ . We have reserved this general setting and its simulation performance to the Supplementary Materials, focusing here on the model shown in Equation (2.5).

## 2.2 Composite Likelihood Function

Specifying the full likelihood function for the proposed model is challenging. Specifically, the joint distribution of  $(I_r, H_r)$  given  $\mathcal{G}_{r-1}$  for  $0 \leq r \leq t$  is difficult to retrieve due to the convolution structure outlined in Equation (2.2), the irregular boundaries and range restrictions applied to  $\{I_r, H_r\}_{0 \leq r \leq t}$ , and the fact that  $h_{t,s}$  are often unobserved in practice. Therefore, we adopt a composite likelihood approach to estimate the model parameters. Specifically, we use joint distribution of  $(I_r, H_r)$  given  $\mathcal{F}_{r-1}$  instead of  $\mathcal{G}_{r-1}$  to construct a composite log-likelihood function

$$\ell_C = \sum_{0 \leq r \leq t} \log \mathbb{P}(H_r, I_r | \mathcal{F}_{r-1}). \quad (2.6)$$



To derive this function, we first demonstrate in the following lemma that  $h_{t,s}$  given  $\mathcal{F}_{t-1}$  follows a Poisson distribution and that  $h_{t,k_1}$  and  $h_{t,k_2}$  are independent given  $\mathcal{F}_{t-1}$  when  $k_1 \neq k_2$ . Then we derive the form of individual component  $\mathbb{P}(H_r, I_r | \mathcal{F}_{r-1})$  based on this lemma.

**Lemma 1** For arbitrary  $t > 0$ ,  $-1 \leq k_1, k_2 \leq \min\{t, \tilde{\eta}\}$  and  $k_1 \neq k_2$ , we have

$$h_{t,k_1} | \mathcal{F}_{t-1} \sim \text{Poisson}(\tilde{\omega}_{k_1} R_t \Lambda_t), \quad h_{t,k_2} | \mathcal{F}_{t-1} \sim \text{Poisson}(\tilde{\omega}_{k_2} R_t \Lambda_t), \quad (2.7)$$

and  $h_{t,k_1} | \mathcal{F}_{t-1} \perp h_{t,k_2} | \mathcal{F}_{t-1}$ . Moreover,  $(h_{t,k_1}, h_{t,k_2}) | \mathcal{G}_{t-1} = (h_{t,k_1}, h_{t,k_2}) | \mathcal{F}_{t-1}$ , and  $h_{t,k_1} | \mathcal{G}_{t-1} \perp h_{t,k_2} | \mathcal{G}_{t-1}$ .

The joint distribution of  $(H_r, I_r)$  and  $\{h_{r-s,s}\}_{1 \leq s \leq \tilde{\eta}}$  conditioning on  $\mathcal{F}_{r-1}$  can be written as

$$\begin{aligned} & \mathbb{P}(H_r, I_r, h_{r-\tilde{\eta},\tilde{\eta}}, \dots, h_{r-1,1} | \mathcal{F}_{r-1}) \\ &= \mathbb{P}\left(h_{r-\tilde{\eta},\tilde{\eta}}, \dots, h_{r-1,1}, h_{r,0} = H_r - \sum_{s=1}^{\tilde{\eta}} h_{r-s,s}, \sum_{s=-1,1,\dots,\tilde{\eta}} h_{r,s} = I_r - H_r + \sum_{s=1}^{\tilde{\eta}} h_{r-s,s} \middle| \mathcal{F}_{r-1}\right). \end{aligned}$$

According to Equation (2.3) and Lemma 1, it can be written as the product of the probability density functions of a few binomial distributions and two Poisson distributions, such that

$$\begin{aligned} & \mathbb{P}(H_r, I_r, h_{r-\tilde{\eta},\tilde{\eta}}, \dots, h_{r-1,1} | \mathcal{F}_{r-1}) \quad (2.8) \\ &= \prod_{s=1}^{\tilde{\eta}} \mathbb{P}\left(\text{Binomial}(I_{r-s}, \tilde{\omega}_s) = h_{r-s,s}\right) \mathbb{1}\left(H_r - I_r \leq \sum_{s=1}^{\tilde{\eta}} h_{r-s,s} \leq H_r\right) \\ & \quad \cdot \mathbb{P}\left(\text{Poisson}(\tilde{\omega}_0 R_r \Lambda_r) = H_r - \sum_{s=1}^{\tilde{\eta}} h_{r-s,s}\right) \\ & \quad \cdot \mathbb{P}\left(\text{Poisson}((1 - \tilde{\omega}_0) R_r \Lambda_r) = I_r - H_r + \sum_{s=1}^{\tilde{\eta}} h_{r-s,s}\right) \end{aligned}$$

Therefore, the joint distribution of  $(H_r, I_r)$  conditioning on  $\mathcal{F}_{r-1}$  can be calculated by summing over all possible values of  $\{h_{r-s,s}\}_{1 \leq s \leq \tilde{\eta}}$  as follows.

$$\mathbb{P}(H_r, I_r | \mathcal{F}_{r-1}) = \sum_{h_{r-\tilde{\eta},\tilde{\eta}}, \dots, h_{r-1,1}} \mathbb{P}(H_r, I_r, h_{r-\tilde{\eta},\tilde{\eta}}, \dots, h_{r-1,1} | \mathcal{F}_{r-1}). \quad (2.9)$$

## 3. INFERENCE

## 3.1 Estimation

In this section, we describe the procedures for estimating model parameters using Monte Carlo expectation–maximization (MCEM) algorithms, treating  $\{h_{r-s,s}\}_{1 \leq s \leq \bar{\eta}}$  as missing data. Let  $\gamma = (\beta, \theta, \omega, \tilde{\omega}) \in \mathbf{\Gamma}$  denote the model parameters, and we use notations like  $\mathbb{P}_\gamma$  to indicate that the probability is associated with the parameter value  $\gamma$ . We use  $\gamma_0$  to denote the parameter values corresponding to the underlying true data-generating mechanism, and  $\hat{\gamma}$  denote the maximum composite likelihood estimator. Let  $D_{obs,r} = \{X_j, I_j\}_{0 \leq j \leq r} \cup \{H_r\}$  denote the observed data and  $D_{miss,r} = \{h_{r-s,s}\}_{1 \leq s \leq \bar{\eta}}$  denote the missing data at time  $r$ . In the MCEM algorithm, we use  $N_0$  to denote the Monte-Carlo sample size, and  $D_{miss,r}^{(m,k)}$ ,  $1 \leq m \leq N_0$  to denote the  $m$ -th Monte-Carlo sample in the  $k$ -th iteration of the EM algorithm. In addition, we use  $\gamma^{(k)}$  to denote the current estimate after the  $k$ -th EM iteration, and similarly, use  $R_r^{(k)}$  and  $\Lambda_r^{(k)}$  to denote the estimates of  $R_r$  and  $\Lambda_r$  based on (2.1) and (2.4) with parameters replaced by  $\gamma^{(k)}$ . The estimation procedure is conceptualized in the following steps and a pseudo-code to implement these steps is shown in Algorithm 1.

**E step** At the  $(k + 1)$ -th iteration, given the current estimate  $\gamma^{(k)} = (\beta^{(k)}, \theta^{(k)}, \omega^{(k)}, \tilde{\omega}^{(k)})$ , this step is to compute the expected complete data composite log-likelihood, or the Q-function, which is defined as

$$Q(\gamma \mid \gamma^{(k)}) \stackrel{\text{def}}{=} \sum_{0 \leq r \leq t} \mathbb{E}_{\gamma^{(k)}} \left( \log \mathbb{P}_\gamma(H_r, I_r, D_{miss,r} \mid \mathcal{F}_{r-1}) \mid D_{obs,r} \right), \quad (3.10)$$

where the expectation is taken with respect to the distribution of  $D_{miss,r}$  conditional on  $(D_{obs,r}, \gamma^{(k)})$ . Due to the computational complexity, the Q-function is calculated using the Monte Carlo method by sampling  $D_{miss,r}$  from  $\mathbb{P}_{\gamma^{(k)}}(D_{miss,r} \mid D_{obs,r})$  and is calculated as

$$\hat{Q}(\gamma \mid \gamma^{(k)}) \stackrel{\text{def}}{=} \sum_{0 \leq r \leq t} \frac{1}{N_0} \sum_{m=1}^{N_0} \log \mathbb{P}_\gamma(H_r, I_r, D_{miss,r}^{(m,k)} \mid \mathcal{F}_{r-1}).$$

**M step** This step is to compute  $\gamma^{(k+1)} = \arg \max_{\gamma \in \Gamma} \hat{Q}(\gamma | \gamma^{(k)})$ . If  $\arg \max_{\gamma \in \Gamma} \hat{Q}(\gamma | \gamma^{(k)})$  is not unique, we randomly choose one as  $\gamma^{(k+1)}$ . When  $\hat{Q}(\gamma^{(k)} | \gamma^{(k)}) = \max_{\gamma \in \Gamma} \hat{Q}(\gamma | \gamma^{(k)})$ , we choose  $\gamma^{(k+1)} = \gamma^{(k)}$ .

It is worth noting that drawing samples from  $P_{\gamma^{(k)}}(D_{\text{miss},r} | D_{\text{obs},r})$  is equivalent to drawing from  $P_{\gamma^{(k)}}(H_r, I_r, D_{\text{miss},r} | \mathcal{F}_{r-1})$  because  $P_{\gamma^{(k)}}(H_r, I_r | \mathcal{F}_{r-1})$  in Equation (2.9) is a constant for a known  $\gamma^{(k)}$ . Therefore, in Algorithm 1, we first draw samples from  $P_{\gamma^{(k)}}(D_{\text{miss},r} | \mathcal{F}_{r-1})$  and accept them with an acceptance rate,  $p_{\text{acceptance}}$ , proportional to  $P_{\gamma^{(k)}}(H_r, I_r | D_{\text{miss},r}, \mathcal{F}_{r-1})$ . In practice, the acceptance rate can be adjusted to accelerate the sampling speed. Specifically, according to Stirling's approximation and the shape of Poisson distributions, we may replace  $p_{\text{acceptance}}$  in Algorithm 1 with

$$p_{\text{acceptance-adj}} = 2\pi R_r^{(k)} \Lambda_r^{(k)} \sqrt{\tilde{\omega}_0^{(k)}(1 - \tilde{\omega}_0^{(k)})} p_{\text{acceptance}}.$$

to improve the algorithm efficiency when the number of infections and hospitalizations is large in the later periods of pandemics.

In Algorithm 1, the parameters of the infectiousness function,  $\omega_s$ , and hospitalization propensity,  $\tilde{\omega}_s$ , are assumed to be unknown. This scenario is often encountered in the early stages of novel pandemics when little is known about the infectious pathogens. However, prior knowledge about  $\omega_s$  and  $\tilde{\omega}_s$  may sometimes be available from multiple biomedical or contact tracing studies. In such scenarios, we may consider these estimates from other studies as prior knowledge. In the Supplementary Materials, we provide another MCEM algorithm, Algorithm 2, to estimate the model parameters when prior knowledge about  $\omega_s$  and  $\tilde{\omega}_s$  is available.

### 3.2 Asymptotic Properties

The basic TSI model (2.1), which describes the generative nature of an infectious pathogen, has many similarities to a branching process. Given that the branching process degenerates on an

---

**Algorithm 1** An MCEM algorithm for estimating the model parameters when both  $\omega_s$  and  $\tilde{\omega}_s$  are unknown.

---

**Require:** initial parameter value  $\gamma^{(0)}$ ,  $k \leftarrow 0$ , breakpoint critical value  $\Delta_0$ .

**while**  $\|\gamma^{(k+1)} - \gamma^{(k)}\|_\infty > \Delta_0$ , **set**  $r \leftarrow 0$ ,  $m \leftarrow 1$ , **do**

**while**  $0 \leq r \leq t$ ,  $1 \leq m \leq N_0$ , **do**

        Sample  $h_{r-s,s}$  independently from Binomial( $I_{r-s}, \tilde{\omega}_s^{(k)}$ ), for  $1 \leq s \leq \tilde{\eta}$ .

        Sample  $\psi$  from Bernoulli distribution with probability  $p_{\text{acceptance}}$ , where

$$p_{\text{acceptance}} = \mathbb{P}\left(\text{Poisson}(\tilde{\omega}_0^{(k)} R_r^{(k)} \Lambda_r^{(k)}) = H_r - \sum_{s=1}^{\tilde{\eta}} h_{r-s,s}\right) \\ \times \mathbb{P}\left(\text{Poisson}((1 - \tilde{\omega}_0^{(k)}) R_r^{(k)} \Lambda_r^{(k)}) = I_r - H_r + \sum_{s=1}^{\tilde{\eta}} h_{r-s,s}\right)$$

**if**  $\psi = 1$ , **then**

$$\text{let } D_{\text{miss},r}^{(m,k)} = \{h_{r-s,s}\}_{1 \leq s \leq \tilde{\eta}}, m \leftarrow m + 1.$$

**end if**

**if**  $m > N_0$ , **then**

$$\text{let } r \leftarrow r + 1, m \leftarrow 1.$$

**end if**

**end while**

    Calculate the Monte Carlo Q-function  $\hat{Q}(\gamma | \gamma^{(k)})$  and  $\gamma^{(k+1)} = \arg \max_{\gamma \in \Gamma} \hat{Q}(\gamma | \gamma^{(k)})$ .

    Let  $k \leftarrow k + 1$ ,  $\hat{\gamma} \leftarrow \gamma^{(k+1)}$ .

**end while**

Output  $\hat{\gamma}$ .

---

extinction set, resulting in no asymptotic property holding for such cases, we similarly define an extinction set  $\mathcal{E}$  for the TSI model,

$$\mathcal{E} \stackrel{\text{def}}{=} \left\{ I_r = 0, \text{ for } r \text{ greater than some } K \right\} = \bigcup_{r \geq 1} \left\{ \frac{\partial \log \mathbb{P}(I_r, H_r | \mathcal{F}_{r-1})}{\partial \gamma} = 0 \right\}, \quad (3.11)$$

and define  $\mathcal{E}_{none} = \mathcal{E}^c$ . Often, no consistent estimator  $\hat{\gamma}$  is anticipated in  $\mathcal{E}$ . Therefore, we set aside the extinction probability

$$\mathbb{P}(\mathcal{E}) = \mathbb{P}\left(\bigcup_{r \geq 1} \left\{ \frac{\partial \log \mathbb{P}(I_r, H_r \mid \mathcal{F}_{r-1})}{\partial \gamma} = 0 \right\}\right)$$

and focus on the asymptotic behavior of  $\hat{\gamma}$  on the non-extinction set  $\mathcal{E}_{none}$ .

In the following theorems, we demonstrate that the ascent property of the composite likelihood function is preserved with the application of the proposed MCEM algorithm and that this algorithm converges for our model. Subsequently, we establish the consistency of the maximum composite likelihood estimator and present it in a practical form of Equation (2.4), subject to certain regularity conditions. Details of the proof can be found in the Supplementary Materials.

**Theorem 1 (Ascent property of the composite likelihood function)** For  $k \geq 0$ , we have  $\ell_C(\gamma^{(k+1)}) \geq \ell_C(\gamma^{(k)})$ .

**Theorem 2 (Convergence of the MCEM-algorithm)** Assume  $\Gamma$  is a compact set, then with  $k \rightarrow \infty$ , the MCEM-estimator  $\gamma^{(k)}$  at the  $k$ -th iteration converges to one of the stationary point  $\gamma_s$  induced by  $M(\cdot) = \arg \max_{\gamma \in \Gamma} Q(\gamma \mid \cdot)$ , and  $\ell_C(\gamma^{(k)})$  converges monotonically to  $\ell_C(\gamma_s)$ .

To demonstrate the consistency of the maximum composite likelihood estimator, we require additional regularity conditions for the behaviors of the observed time series. Drawing inspiration from pioneering work in counting process (Zeger, 1988; Zeger and Qaqish, 1988; Davis *and others*, 1999, 2000, 2003; Fokianos *and others*, 2009; Neumann *and others*, 2011; Doukhan *and others*, 2012), we first assume

**Condition 1 (Series ergodicity)** There exist  $t_0 > 0$ , such that,

$$\lim_{t \rightarrow \infty} \frac{t_0}{t} \sum_{s=1}^t R_s \Lambda_s \rightarrow_{a.s.} \sum_{s=1}^{t_0} \mathbb{E} R_s \Lambda_s, \quad \lim_{t \rightarrow \infty} \frac{t_0}{t} \sum_{s=1}^t I_s \log(R_s) \rightarrow_{a.s.} \sum_{s=1}^{t_0} \mathbb{E} I_s \log(R_s).$$

We also assume that the time series regression, represented by Equation (2.4), uses a log

link function and is characterized as an autoregressive model of order 1, such that  $\log(R_t) = Z_t^T \beta + \theta_0 + \theta_1 \log(R_{t-1})$ . We then establish the consistency of the maximum composite likelihood estimator for the time series regression coefficients when the infectiousness function and hospitalization propensity,  $(\omega_s, \tilde{\omega}_s)$ , are known. We denote the parameters of interest as  $\gamma|_\omega = (\beta, \theta)$ . The consistency of the maximum composite likelihood estimator,  $\hat{\gamma}|_\omega = (\hat{\beta}, \hat{\theta})$ , is shown as follows.

**Theorem 3 (Strong consistency of the estimators)** Under condition 1 and assuming that  $\Gamma$  is a compact set, we have  $\hat{\gamma}|_\omega \xrightarrow{a.s.} \gamma_0|_\omega$  as the length of the observational days  $t \rightarrow \infty$ ,

where  $\gamma_0|_\omega$  is the parameter value corresponding to the true data generating mechanism. Furthermore, with the following conditions from the theorem 3 of Kaufmann (1987), that is

**Condition 2 (Non-singularity)** For each  $1 \leq r \leq t$ , define

$$\xi_r(\gamma|_\omega) = \frac{\partial R_r}{\partial \gamma|_\omega} \cdot R_r^{-1} \cdot (I_r - R_r \Lambda_r).$$

There exists some nonrandom and non-singular normalizing matrix  $A_t$ , such that the normalized conditional variance converges to an almost surely positive definite random matrix  $\zeta^T \zeta$ , i.e.,

$$A_t^{-1} \left[ \sum_{r=1}^t \text{Cov}(\xi_r(\gamma_0|_\omega) \mid \mathcal{F}_{r-1}) \right] (A_t^{-1})^T \xrightarrow{P} \zeta^T \zeta.$$

**Condition 3 (Uniformly integrability)** For  $1 \leq r \leq t$ ,  $\mathbb{E}[\xi_r^2(\gamma_0) \mid \mathcal{F}_{r-1}]$  is termwise uniformly integrable.

**Condition 4 (The conditional Lindeberg condition)** For arbitrary  $\epsilon > 0$ ,

$$\sum_{r=1}^t \mathbb{E} \left[ \xi_r^T(\gamma_0|_\omega) (A_t^T A_t)^{-1} \xi_r(\gamma_0|_\omega) \cdot \mathbb{1}(|\xi_r^T(\gamma_0|_\omega) (A_t^T A_t)^{-1} \xi_r(\gamma_0|_\omega)| > \epsilon^2) \mid \mathcal{F}_{r-1} \right] \xrightarrow{P} 0.$$

**Condition 5 (The smoothness condition)** For arbitrary  $\delta > 0$ , and  $\delta$ -neighborhood ball  $\mathcal{B}_t(\delta)$  defined as  $\mathcal{B}_t(\delta) = \{\tilde{\gamma}|_\omega : \|A_t^T(\tilde{\gamma}|_\omega - \gamma_0|_\omega)\| \leq \delta\}$ ,

$$\sup_{\tilde{\gamma}|_\omega \in \mathcal{B}_t(\delta)} \left\| A_t^{-1} \sum_{r=1}^t \left( \frac{\partial \xi_r(\tilde{\gamma}|_\omega)}{\partial \gamma} + \text{Cov}(\xi_r(\gamma_0|_\omega) \mid \mathcal{F}_{r-1}) \right) (A_t^{-1})^T \right\| \xrightarrow{P} 0.$$

the maximum composite likelihood estimator converges to a normal distribution as shown below.

**Theorem 4 (Asymptotic normality)** Under condition 1-5, and assume  $\Gamma$  is a compact set, then on the non-extinction set defined in (3.11), with  $t \rightarrow \infty$ ,

$$\left[ \sum_{r=1}^t \text{Cov}(\xi_r(\gamma_0|\omega) \mid \mathcal{F}_{r-1}) \right]^{1/2} (\hat{\gamma}|\omega - \gamma_0|\omega) \xrightarrow{d} N(0, I), \quad (3.12)$$

where  $I$  is the identify matrix.

## 4. SIMULATION STUDIES

### 4.1 Simulation Setups

To evaluate the performance of the proposed method, we conducted several simulation studies under two sets of scenarios. In the first set of scenarios, the reported counts of new infections represent the true number of new infections, indicating that the TSI model for the generation of new infections is correctly specified (correctly specified model). In the second set of scenarios, the reported numbers of new infections contain errors due to under-reporting, limited testing or any other reporting errors, implying that the TSI model is misspecified (misspecified model). In all scenarios, we assumed the hospitalization data to be accurate. Each scenario was repeated for 1,000 replications to calculate the bias and coverage probability of the proposed estimator.

In the simulations, data on daily new infections, hospital admissions, and the covariates associated with disease transmission are generated from the proposed model (2.1)-(2.5), with (2.4) simplified as  $\log(R_r) = Z_r^T \beta + \theta_0 + \theta_1 \log(R_{r-1})$ , for  $r \geq 1$ , which means that the logarithm of the instantaneous reproduction number  $\{R_r\}_{1 \leq r \leq t}$ , follows an AR(1) structure with exogenous terms. Following the results in an earlier study by Li *and others* (2020), we configured the infectiousness function and the hospitalization propensity as follows

$$\omega_s = \mathbb{P}(\Gamma(k_1, \mu_1) \in [s - 1, s]), \quad s = 1, \dots, 24, \quad \text{and} \quad \omega_{25} = \mathbb{P}(\Gamma(k_1, \mu_1) \geq 24),$$

$$2\tilde{\omega}_s = \mathbb{P}(\Gamma(k_2, \mu_2) \in [s, s + 1]), \quad s = 0, \dots, 4, \quad 2\tilde{\omega}_5 = \mathbb{P}(\Gamma(k_2, \mu_2) \geq 5), \quad \text{and} \quad \tilde{\omega}_{-1} = 0.5,$$

with the Gamma distributions  $\Gamma(\cdot, \cdot)$  having shape parameters  $k_1 = 2.5$ ,  $k_2 = 1.6$ , and scale parameters  $\mu_1 = 3$ ,  $\mu_2 = 1.5$ . We set the study duration  $T = 120$  and fixed  $p = 2$ . Parameter values were assigned as  $(\theta_0, \theta_1, \beta^T) = (0.7, 0.5, -.02, -.125)$ . We independently simulated the two sequences of covariates  $\{Z_{r,1}, Z_{r,2}\}_{1 \leq r \leq t}$  to emulate real data on temperature in Philadelphia and social distancing data derived from daily cellular telephone movements, as provided by Unacast Unacast (1st). This data represented the percentage change in visits to non-essential businesses, such as restaurants and hair salons, between March 1st and June 30th, 2020.

#### 4.2 Simulation Results with Correctly Specified Model

In this set of scenarios, we explored three circumstances and compared the model's performance against the reference approach by Cori *and others* (2013). In the first circumstance, we assumed the infectiousness function  $\omega_s$  and hospitalization propensity  $\tilde{\omega}_s$  were known. The model parameters were reduced to  $\gamma = (\theta^T, \beta^T)$ . For the reference approach, we selected the sliding window by minimizing the  $\mathcal{L}_2$ -distance of the estimated and oracle sequence of  $\{R_r\}_{1 \leq r \leq t}$ . For the proposed method, we selected the initial  $\gamma^{(0)}$  randomly and away from the oracle value. Figure 2 demonstrates the estimation bias of  $\{R_r\}_{1 \leq r \leq t}$  for both methods. We found that both methods could capture the trend of  $\{R_r\}_{1 \leq r \leq t}$  well with a very small estimation bias, but the proposed method performed better than the baseline method with a smaller bias. Moreover, when  $\omega_s$  and  $\tilde{\omega}_s$  were known, we found the proposed MCEM algorithm converged very fast, and the estimation bias for  $\{R_r\}_{1 \leq r \leq t}$  reached its limit after only two iterations of running the algorithm. In the second circumstance, we assumed that  $\omega_s$  and  $\tilde{\omega}_s$  were unknown but prior knowledge about  $\omega_s$  was available. We used the estimated infectiousness functions from previous studies as the prior knowledge, (Wu *and others*, 2020; Ali *and others*, 2020; Chen *and others*, 2022; Deng *and others*, 2021), set the true function according to the results in Li *and others* (2020), and used Algorithm 2 to estimate the parameters. The results were similar to those observed in the first



circumstance when  $\omega_s$  and  $\tilde{\omega}_s$  were known, except for a small increase in estimation bias for both approaches. In the third circumstance, we assumed that  $\omega_s$  and  $\tilde{\omega}_s$  were unknown and no prior knowledge was available. In this situation, we only estimated the parameters using the proposed method, since the reference approach either requires user-specified values to constrain the overall shape of the infectiousness function or needs user-provided contact tracking data to estimate the infectiousness function. Using the proposed method, we estimated the regression coefficients as well as the infectiousness function and hospitalization propensity. As shown in Table.1, the proposed method produced accurate estimates for parameters with small bias and good coverage probability. The method also consistently estimated the instantaneous reproduction numbers, as shown in Figure 3. Overall, when the TSI model is correctly specified, the proposed composite likelihood MCEM algorithm benefits from incorporating hospital admission data, outperforming the reference approach.

Table 1. Performance of the proposed method when the reported number of daily new infections was accurate, the infectiousness function  $\omega_s$  and hospitalization propensity  $\tilde{\omega}_s$  were unknown and no prior knowledge was available. For  $\omega_s$  and  $\tilde{\omega}_s$ , only estimates of selected parameters are presented, due to the large number of parameters. Estimates of the other parameters not shown here yield similar results.

	$\theta_0$	$\theta_1$	$\beta_1$	$\beta_2$	$\omega_5$	$\omega_6$	$\tilde{\omega}_0$
Empirical bias ( $\times 10^{-3}$ )	-0.15	2.10	0.08	0.15	-0.45	-0.40	-0.04
Relative bias ( $\times 10^{-3}$ )	-0.22	4.20	-3.79	-1.23	-4.40	-4.01	-0.32
Standard error( $\times 10^{-3}$ )	6.29	3.34	0.23	0.39	2.23	2.29	0.60
95% Coverage probability	94.6%	92.0%	94.2%	96.2%	96.2%	97.0%	94.4%

### 4.3 Simulation Results with Misspecified Model

In the second sets of scenarios, we assumed the reported number of daily new infections was not accurate. In these scenarios, only a proportion of true infections were reported, and this proportion varied from day to day. We generated the daily proportion of unreported infections from a normal distribution with mean and standard deviation equal to 15% and 5%, respectively. This allowed the daily under-reporting proportion to vary from 0% to 30%, resulting in poor data

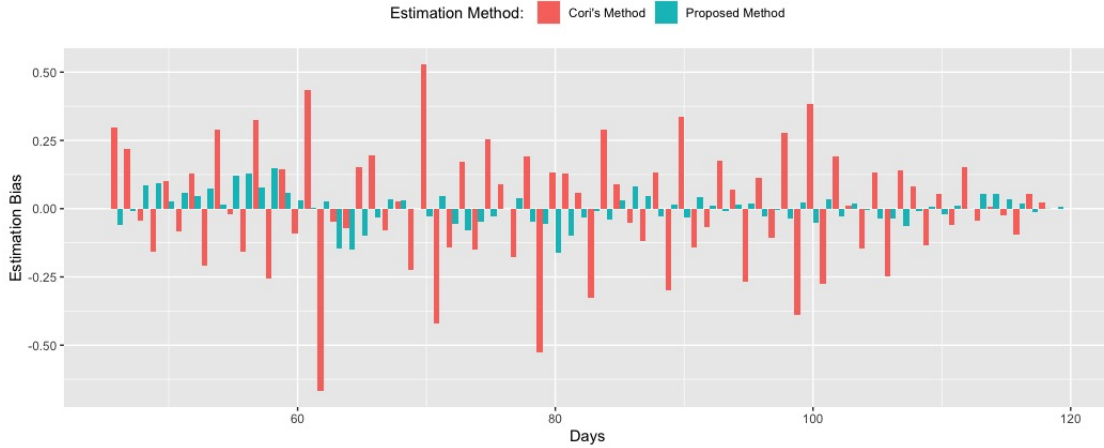


Fig. 2. Comparison of the estimation bias in the daily instantaneous reproduction number,  $R_t$ , between the proposed method and Cori's method (Cori *and others*, 2013) when the reported number of daily new infections was accurate, and both the infectiousness function  $\omega_s$  and hospitalization propensity  $\tilde{\omega}_s$  were known. The estimation bias was calculated as the difference between the estimated daily  $R_t$  and the oracle  $R_t$  that generates the data.

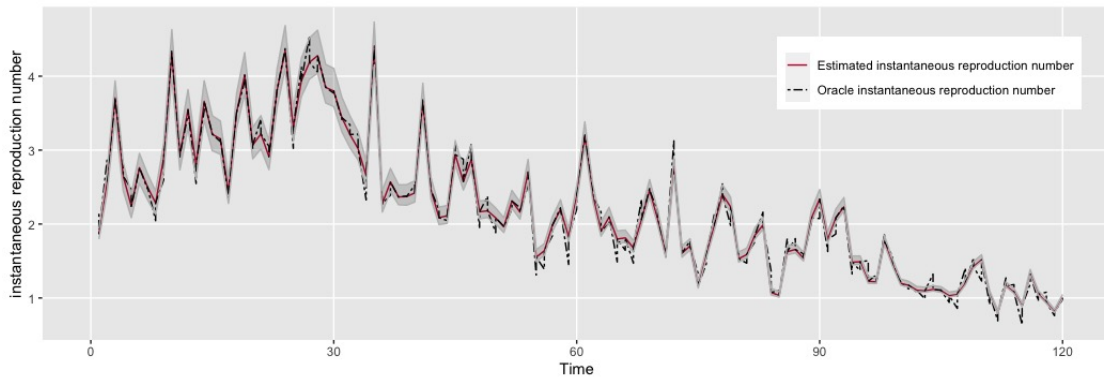


Fig. 3. Estimation of the daily instantaneous reproduction number,  $R_t$ , when the reported number of daily new infections was accurate, the infectiousness function  $\omega_s$  and hospitalization propensity  $\tilde{\omega}_s$  were unknown and no prior knowledge was available. Black dotted line stands for the oracle  $R_t$ . Red solid line and the grey shadow stand for the estimates and its corresponding Bootstrapping confidence interval using the proposed method.

quality for the reported infection numbers. However, we assumed the daily hospital admission data were accurate, ensuring that all hospitalized patients were reported and documented in a timely manner.

Given the oracle instantaneous reproduction number, we simulated the number of true daily infections, the underreporting proportion, and hospital admission data in each replication. We calculated parameter estimates and the instantaneous reproduction number using the proposed method. We found that the performance was very similar to the correctly specified model scenario shown in Table 1. For example, the mean of the point estimates for  $\beta$  was very close to the estimated parameter value  $(-0.0206, -0.1239)$  in the mis-specified model, compared to  $(-0.02, -0.125)$  in the correctly specified model. However, the standard error for  $\beta$  was higher in the mis-specified model scenario  $(0.003, 0.009)$  compared to the correctly specified model  $(0.0003, 0.0004)$ . We also compared the results with another recently proposed method that used a measurement error model to account for the data errors in the reported infections (Shi *and others*, 2022). We found that although both methods reduced the bias induced by data errors, the proposed method performed slightly better than Shi *and others* (2022), providing more accurate estimates of the instantaneous reproduction number, as shown in Figure 4.

## 5. APPLICATION TO COVID-19 DATA

We applied the proposed method to a COVID-19 dataset comprising daily reported infections and hospital admissions from January 1st to June 30th, 2021, across four counties: Miami-Dade, FL; New York, NY; Cook (Chicago), IL; and Wayne (Detroit), MI. These counties represent four major metropolitan areas in the Southeast coast, Tri-State area, and Great Lakes region of the United States. We obtained county-level data on daily new infections and hospitalizations due to COVID-19 from the National Healthcare Safety Network (NHSN) database. Additionally, two county-level variables were sourced: daily social distancing practices, indicated by the percentage

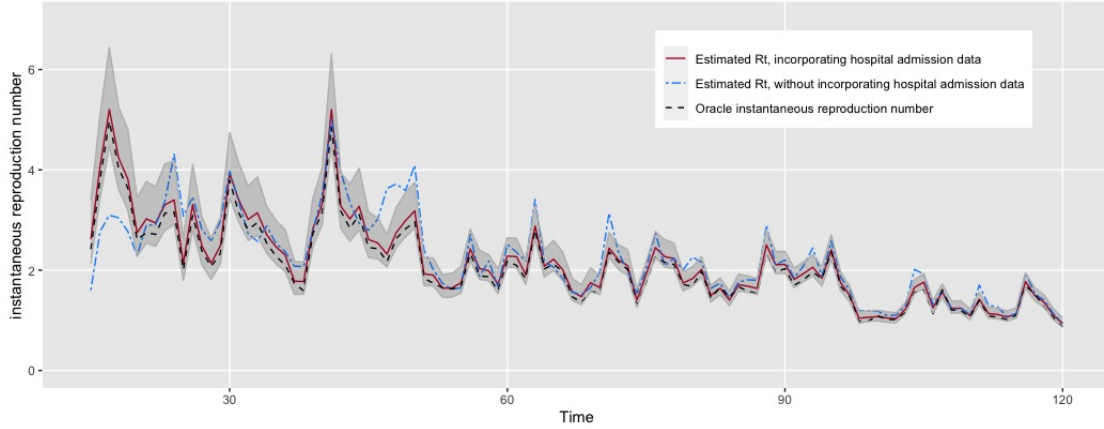


Fig. 4. Estimation of the instantaneous reproduction number when the daily new infections were reported with 0%-30% under-reporting rates. Black dotted line stands for the oracle instantaneous reproduction number. Red solid line and the gray shadow stand for the estimates and its corresponding Bootstrapping confidence interval using the proposed method. Blue dashed line stands for the estimates using a comparison method (Shi *and others*, 2022).

change in visits to nonessential businesses (from Unacast), and wet-bulb temperature (from the National Oceanic and Atmospheric Administration). Our objectives included estimating the daily instantaneous reproduction number  $R_t$ , the infectiousness function  $\omega_s$ , and the hospitalization propensity  $\tilde{\omega}_s$  of COVID-19 during the study period. We also aimed to evaluate the association between county-level factors and COVID-19 disease transmission. Our findings are intended to provide evidence supporting the selection of appropriate public health policies and guide health resource allocation in each county.

When fitting the proposed model, we allowed the hospitalization propensity to vary by county considering differential health resources and access to healthcare across the four counties. In addition, given the limitations of the US COVID-19 disease surveillance data, which record incidence at the time of disease diagnosis rather than actual infection and considering that the exact infection times are rarely known, we interpret the infectiousness function and hospitalization propensity estimated from this data based on the diagnosis time rather than infection

time. Specifically, we designated  $\tilde{\omega}_{-1,c}$  and  $\tilde{\omega}_{s,c}$  to represent the propensities of never becoming hospitalized and being hospitalized on the  $s$ -th day after diagnosis, respectively, for each county with  $c \in \{1, 2, 3, 4\}$ . This specification facilitates modeling heterogeneity across counties. We also assume the  $\omega_s$  reflects the infectiousness of the existing infectious individuals on the  $s$ -th day after diagnosis. We employed the block approach (Bühlmann and Künsch, 1999; Bühlmann, 2002; Hall, 1985; Künsch, 1989) to calculate the bootstrap confidence interval. Additionally, the fitted time series structure (2.4) was determined by data using AIC among the family of autoregressive models with exogenous terms. The lengths of the infectiousness function and hospitalization propensity,  $\eta$  and  $\tilde{\eta}$ , were directly determined by maximizing the composite likelihood.

The final model selected was the same as the AR(1) model used in the simulation study. The  $\eta$  and  $\tilde{\eta}$  were estimated to be 22 and 4, respectively. The estimated effect sizes for social distancing and wet-bulb temperature were 0.1539, with a 95% confidence interval of (0.1537, 0.1541), and  $-7.3 \times 10^{-4}$ , with a 95% confidence interval of  $(-8.3 \times 10^{-4}, -6.4 \times 10^{-4})$ , respectively. These results suggested that lack of social distancing was a strong risk factor for elevated disease transmission during the study period. For example, a 50% reduction in the frequency of visiting non-essential businesses was estimated to reduce  $R_t$  by an average of 7.4%. On the contrary, temperature exerted only a minor effect on disease transmission during the study period. The estimated county-level  $R_t$  exhibited a similar trend during the study period among all four counties, as depicted in Figure 5. A decrease in disease transmission was observed since April 2021, which, in this dataset, was largely attributed to a reduction in social distancing value. Figure 6 illustrates the estimated infectiousness function. The shape of the infectiousness functions resembled the probability density function of either a Gamma or Weibull distribution (Figure 6a), with nearly two-thirds of secondary infections being diagnosed within the first week after the diagnosis of the infectors (Figure 6b). If we assume that the duration between infection and diagnosis is roughly the same for both infectors and secondary infections, our finding suggests that timely

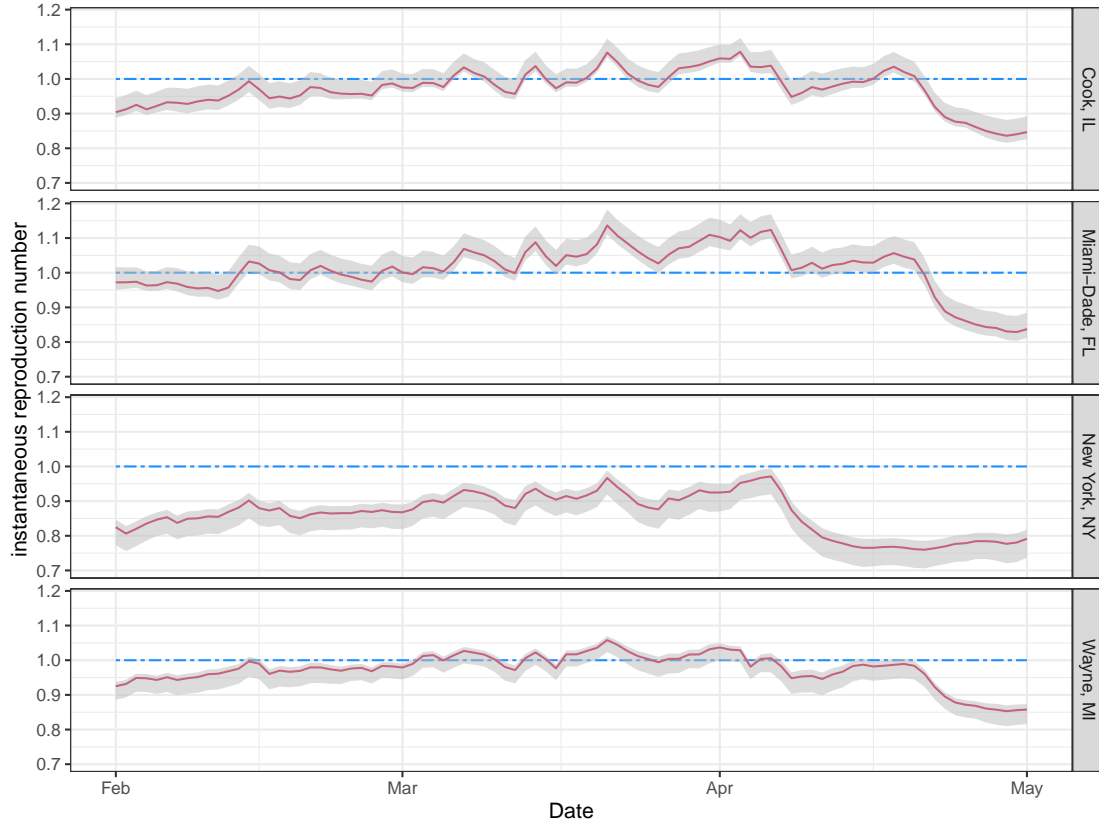


Fig. 5. Estimated instantaneous reproduction number,  $R_t$ , for COVID-19 in the four studied counties during February to May 2021. The blue lines represent the critical value of  $R_t = 1$ . Red lines represent the estimated county-level  $R_t$  during the study period. Shaded areas indicate the bootstrap confidence intervals.

testing and a subsequent week-long quarantine of infected individuals can significantly mitigate disease transmission.

The estimated hospitalization propensity for each county is presented in Figure 7. Given the varied access to healthcare, hospitalization propensity diverged across locations. In New York, the propensity for hospitalization sometime after diagnosis was highest among the four studied counties, slightly lower than 20%, compared to about 10% in Miami (Figure 7b). The propensity for hospitalization on the first day of diagnosis was also highest in New York, at approximately

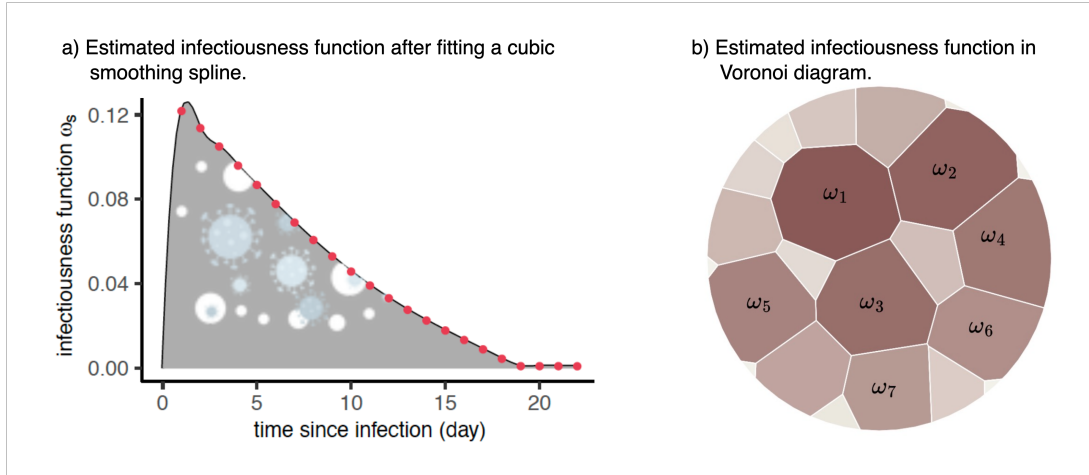


Fig. 6. Visualization of the estimated infectiousness function,  $\omega_s$ , for COVID-19 in the four studied counties during February to May 2021. In panel a), the red dots represent the estimated  $\omega_s$ ,  $1 \leq s \leq 22$ , while the black line represents the estimated infectiousness function after fitting a cubic smoothing spline. In panel b), the estimated  $\omega_s$  values are visualized using a Voronoi diagram to compare the magnitude of each  $\omega_s$ . Values of  $\omega_s$  in the first week since infection are labeled.

15.5% (Figure 7b), compared to less than 5% in Miami or Cook. Despite these differences, we found that most hospitalizations occurred within 4 days after a COVID-19 diagnosis, and the mean time from diagnosis to hospital admission was around 1 day in all four counties. Assuming it takes, on average, 48 hours from symptom onset to diagnosis, then most COVID-19 hospitalizations occurred within 6 days after symptom onset, and the mean time from symptom onset to hospital admission is around 3 days. These results generated from our analysis are consistent with findings from other COVID-19 studies based on different cohorts. For example, a CDC report showed that 20.9% diagnosed COVID-19 patients in US were hospitalized before March 28, 2020 (Team *and others*, 2020). Zhang *and others* (2020) studied patients from early Hubei, China, for COVID patients during Jan 19 to Feb 17, 2020. They found that the mean time from symptom onset to hospital admission decreased from 4.4 days (95% CI 0.0–14.0) for the period of Dec 24 to Jan 27, to 2.6 days (0.0–9.0) for the period of Jan 28 to Feb 17. These estimates of COVID-19

hospitalizations are important and can inform hospital planning. However, traditionally, studying such durations requires epidemiological studies with contact tracing data, which poses a high requirement for the US disease surveillance system. Our study demonstrates that our method can utilize US disease surveillance data to estimate these parameters.

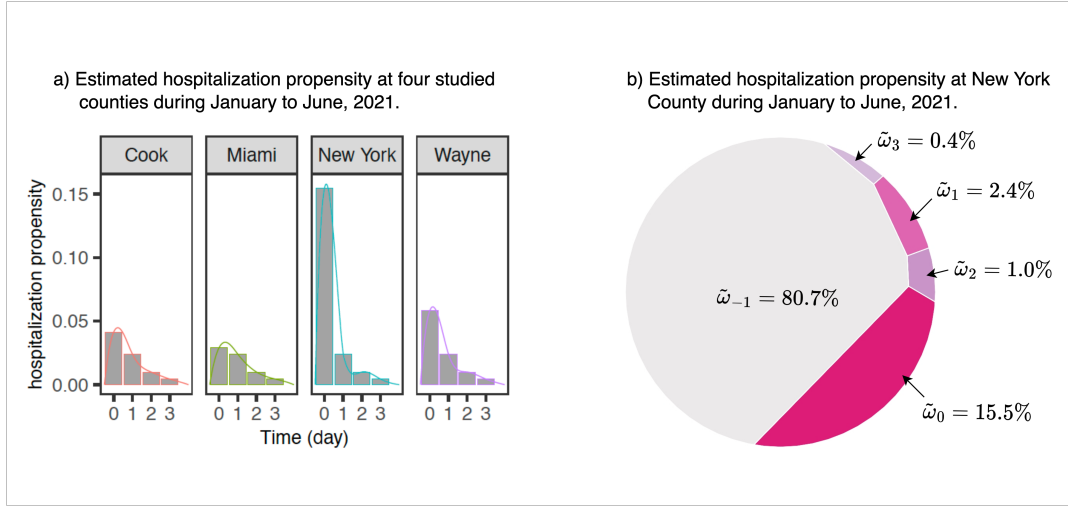


Fig. 7. Visualization of the estimated hospitalization propensity,  $\tilde{\omega}_s$ , for COVID-19 in the four studied counties during February to May 2021. In panel a), the bar plot shows the estimated value of  $\tilde{\omega}_s$ ,  $1 \leq s \leq 4$ , at the four studied counties, while the solid lines represent the estimated propensity after fitting a cubic smoothing spline. In panel b), the estimated  $\tilde{\omega}_s$  values at New York County are visualized using a Voronoi diagram to compare the magnitude of each  $\tilde{\omega}_s$ . Most of the hospitalized patients were admitted to a hospital on the day of infection.

## 6. DISCUSSION

Given the existing importance of the TSI model in studying infectious diseases, the proposed method and algorithm elevate its usefulness and potential to a higher level. The proposed model not only enhances the robustness of the TSI model by incorporating hospitalization data but also enables investigations into infectiousness functions and hospitalization propensities. This, in turn, facilitates the prediction of hospitalization using the TSI model.



The proposed method can be extended in several ways. First, the framework can be expanded to incorporate additional data elements, such as disease-related daily death counts, PCR tests, and serological data, aiming to further enhance the accuracy of parameter estimates and enable the modeling and prediction of death counts. Second, the proposed method does not take into account potential spatial correlations between locations in disease transmission. Traffic data can be utilized to construct a correlation matrix for modeling such correlations, thus improving the model's efficiency. Third, the evolution of infectious pathogens and changes in immunity due to infections and vaccinations can alter the dynamics of disease transmission. The proposed method can be extended to study different variants of the virus and assess the impact of population immunity on disease transmission. Fourth, the model can be expanded to accommodate overdispersion in daily infection numbers or reduce parametric assumptions through method constraints.

## REFERENCES

- ALI, SHEIKH TASLIM, WANG, LIN, LAU, ERIC HY, XU, XIAO-KE, DU, ZHANWEI, WU, YE, LEUNG, GABRIEL M AND COWLING, BENJAMIN J. (2020). Serial interval of sars-cov-2 was shortened over time by nonpharmaceutical interventions. *Science* **369**(6507), 1106–1109.
- AMMAN, FABIAN, MARKT, RUDOLF, ENDLER, LUKAS, HUPFAUF, SEBASTIAN, AGERER, BENEDIKT, SCHEDL, ANNA, RICHTER, LUKAS, ZECHMEISTER, MELANIE, BICHER, MARTIN, HEILER, GEORG *and others*. (2022). Viral variant-resolved wastewater surveillance of sars-cov-2 at national scale. *Nature biotechnology* **40**(12), 1814–1822.
- BÜHLMANN, PETER. (2002). Bootstraps for time series. *Statistical science*, 52–72.
- BÜHLMANN, PETER AND KÜNSCH, HANS R. (1999). Block length selection in the bootstrap for time series. *Computational Statistics & Data Analysis* **31**(3), 295–310.
- CHEN, DONGXUAN, LAU, YIU-CHUNG, XU, XIAO-KE, WANG, LIN, DU, ZHANWEI, TSANG,

- TIM K, WU, PENG, LAU, ERIC HY, WALLINGA, JACCO, COWLING, BENJAMIN J *and others*. (2022). Inferring time-varying generation time, serial interval, and incubation period distributions for covid-19. *Nature communications* **13**(1), 7727.
- CORI, ANNE. (2021). *EpiEstim: Estimate Time Varying Reproduction Numbers from Epidemic Curves*. R package version 2.2-4.
- CORI, ANNE, FERGUSON, NEIL M, FRASER, CHRISTOPHE AND CAUCHEMEZ, SIMON. (2013). A new framework and software to estimate time-varying reproduction numbers during epidemics. *American journal of epidemiology* **178**(9), 1505–1512.
- DAVIS, RICHARD A, DUNSMUIR, WILLIAM TM AND STREETT, SARAH B. (2003). Observation-driven models for poisson counts. *Biometrika* **90**(4), 777–790.
- DAVIS, RICHARD A, DUNSMUIR, WILLIAM TM AND WANG, YING. (1999). Modeling time series of count data. *Statistics Textbooks and Monographs* **158**, 63–114.
- DAVIS, RICHARD A, DUNSMUIR, WILLIAM TM AND WANG, YIN. (2000). On autocorrelation in a poisson regression model. *Biometrika* **87**(3), 491–505.
- DENG, YUHAO, YOU, CHONG, LIU, YUKUN, QIN, JING AND ZHOU, XIAO-HUA. (2021). Estimation of incubation period and generation time based on observed length-biased epidemic cohort with censoring for covid-19 outbreak in china. *Biometrics* **77**(3), 929–941.
- DOUKHAN, PAUL, FOKIANOS, KONSTANTINOS AND TJØSTHEIM, DAG. (2012). On weak dependence conditions for poisson autoregressions. *Statistics & Probability Letters* **82**(5), 942–948.
- FOKIANOS, KONSTANTINOS, RAHBEK, ANDERS AND TJØSTHEIM, DAG. (2009). Poisson autoregression. *Journal of the American Statistical Association* **104**(488), 1430–1439.
- FRASER, CHRISTOPHE. (2007). Estimating individual and household reproduction numbers in an emerging epidemic. *PloS one* **2**(8), e758.

- GE, YONG, WU, XILIN, ZHANG, WENBIN, WANG, XIAOLI, ZHANG, DIE, WANG, JIANGHAO, LIU, HAIYAN, REN, ZHOUPENG, RUKTANONCHAI, NICK W, RUKTANONCHAI, CORRINE W *and others.* (2023). Effects of public-health measures for zeroing out different sars-cov-2 variants. *Nature Communications* **14**(1), 5270.
- GOSTIC, KATELYN M, MCGOUGH, LAUREN, BASKERVILLE, EDWARD B, ABBOTT, SAM, JOSHI, KEYA, TEDIJANTO, CHRISTINE, KAHN, REBECCA, NIEHUS, RENE, HAY, JAMES A, DE SALAZAR, PABLO M *and others.* (2020). Practical considerations for measuring the effective reproductive number,  $r_t$ . *PLoS computational biology* **16**(12), e1008409.
- HALL, PETER. (1985). Resampling a coverage pattern. *Stochastic processes and their applications* **20**(2), 231–246.
- JEWELL, NICHOLAS P. (2021). Statistical models for covid-19 incidence, cumulative prevalence, and  $r_t$ . *Journal of the American Statistical Association* **116**(536), 1578–1582.
- KAUFMANN, HEINZ. (1987). Regression models for nonstationary categorical time series: asymptotic estimation theory. *The Annals of Statistics*, 79–98.
- KERMACK, WILLIAM OGILVY AND MCKENDRICK, ANDERSON G. (1927). A contribution to the mathematical theory of epidemics. *Proceedings of the royal society of london. Series A, Containing papers of a mathematical and physical character* **115**(772), 700–721.
- KÜNSCH, HANS R. (1989). The jackknife and the bootstrap for general stationary observations. *Annals of Statistics* **17**(3), 1217–1241.
- LI, QUN, GUAN, XUHUA, WU, PENG, WANG, XIAOYE, ZHOU, LEI, TONG, YEQING, REN, RUIQI, LEUNG, KATHY SM, LAU, ERIC HY, WONG, JESSICA Y *and others.* (2020). Early transmission dynamics in wuhan, china, of novel coronavirus–infected pneumonia. *New England journal of medicine*.

- NASH, REBECCA K, NOUVELLET, PIERRE AND CORI, ANNE. (2022). Real-time estimation of the epidemic reproduction number: Scoping review of the applications and challenges. *PLOS Digital Health* **1**(6), e0000052.
- NEUMANN, MICHAEL H *and others*. (2011). Absolute regularity and ergodicity of poisson count processes. *Bernoulli* **17**(4), 1268–1284.
- NOUVELLET, PIERRE, BHATIA, SANGEETA, CORI, ANNE, AINSLIE, KYLIE EC, BAGUELIN, MARC, BHATT, SAMIR, BOONYASIRI, ADHIRATHA, BRAZEAU, NICHOLAS F, CATTARINO, LORENZO, COOPER, LAURA V *and others*. (2021). Reduction in mobility and covid-19 transmission. *Nature communications* **12**(1), 1090.
- PAN, AN, LIU, LI, WANG, CHAOLONG, GUO, HUAN, HAO, XINGJIE, WANG, QI, HUANG, JIAO, HE, NA, YU, HONGJIE, LIN, XIHONG *and others*. (2020). Association of public health interventions with the epidemiology of the covid-19 outbreak in wuhan, china. *Jama* **323**(19), 1915–1923.
- QUICK, CORBIN, DEY, ROUNAK AND LIN, XIHONG. (2021). Regression models for understanding covid-19 epidemic dynamics with incomplete data. *Journal of the American Statistical Association* **116**(536), 1561–1577.
- ROSS, RONALD. (1916). An application of the theory of probabilities to the study of a priori pathometry.—part i. *Proceedings of the Royal Society of London. Series A, Containing papers of a mathematical and physical character* **92**(638), 204–230.
- ROSS, RONALD AND HUDSON, HILDA P. (1917a). An application of the theory of probabilities to the study of a priori pathometry.—part ii. *Proceedings of the Royal Society of London. Series A, Containing papers of a mathematical and physical character* **93**(650), 212–225.
- ROSS, RONALD AND HUDSON, HILDA P. (1917b). An application of the theory of probabilities

- to the study of a priori pathometry.—part iii. *Proceedings of the Royal Society of London. Series A, Containing papers of a mathematical and physical character* **93**(650), 225–240.
- SALAS, JOAQUIN. (2021). Improving the estimation of the covid-19 effective reproduction number using nowcasting. *Statistical Methods in Medical Research* **30**(9), 2075–2084.
- SHI, JIASHENG, MORRIS, JEFFREY S, RUBIN, DAVID M AND HUANG, JING. (2022). Robust modeling and inference of disease transmission using error-prone data with application to sars-cov-2. *arXiv preprint arXiv:2212.08282*.
- SVENSSON, ÅKE. (2007). A note on generation times in epidemic models. *Mathematical biosciences* **208**(1), 300–311.
- TEAM, CDC COVID-19 RESPONSE, TEAM, CDC COVID-19 RESPONSE, TEAM, CDC COVID-19 RESPONSE, CHOW, NANCY, FLEMING-DUTRA, KATHERINE, GIERKE, RYAN, HALL, ARON, HUGHES, MICHELLE, PILISHVILI, TAMARA, RITCHEY, MATTHEW *and others*. (2020). Preliminary estimates of the prevalence of selected underlying health conditions among patients with coronavirus disease 2019—united states, february 12–march 28, 2020. *Morbidity and mortality weekly report* **69**(13), 382–386.
- UNACAST. (2021, July 1st). Social distancing scoreboard.
- WALLINGA, JACCO AND TEUNIS, PETER. (2004). Different epidemic curves for severe acute respiratory syndrome reveal similar impacts of control measures. *American Journal of epidemiology* **160**(6), 509–516.
- WHO EBOLA RESPONSE TEAM. (2014). Ebola virus disease in west africa—the first 9 months of the epidemic and forward projections. *New England Journal of Medicine* **371**(16), 1481–1495.
- WILDER, BRYAN, MINA, MICHAEL AND TAMBE, MILIND. (2021). Tracking disease outbreaks

- from sparse data with bayesian inference. In: *Proceedings of the AAAI Conference on Artificial Intelligence*, Volume 35. pp. 4883–4891.
- WU, JOSEPH T, LEUNG, KATHY, BUSHMAN, MARY, KISHORE, NISHANT, NIEHUS, RENE, DE SALAZAR, PABLO M, COWLING, BENJAMIN J, LIPSITCH, MARC AND LEUNG, GABRIEL M. (2020). Estimating clinical severity of covid-19 from the transmission dynamics in wuhan, china. *Nature medicine* **26**(4), 506–510.
- ZEGER, SCOTT L. (1988). A regression model for time series of counts. *Biometrika* **75**(4), 621–629.
- ZEGER, SCOTT L AND QAQISH, BAHJAT. (1988). Markov regression models for time series: a quasi-likelihood approach. *Biometrics*, 1019–1031.
- ZHANG, JUANJUAN, LITVINOVA, MARIA, WANG, WEI, WANG, YAN, DENG, XIAOWEI, CHEN, XINGHUI, LI, MEI, ZHENG, WEN, YI, LAN, CHEN, XINHUA *and others*. (2020). Evolving epidemiology and transmission dynamics of coronavirus disease 2019 outside hubei province, china: a descriptive and modelling study. *The Lancet Infectious Diseases* **20**(7), 793–802.